Can. J. Remote Sensing, Vol. 28, No. 3, pp. 346–353, 2002

Applying a unified directional wave spectrum to the remote sensing of wind wave directional spreading

Malcolm L. Heron

Abstract. Models for directional wind wave spectra can be used to assist in interpretation and analysis of Doppler sea echo spectra to determine wind direction over the oceans by remote sensing techniques. This paper compares and contrasts the data analysis required at different electromagnetic wavelengths. At large wavenumbers the observed spreading depends not only on the directional spreading at the Bragg wavenumber, but also on the weighted integrals over all shorter wavenumbers. This is discussed in terms of microwave and VHF Doppler spectra. At small wavenumbers (HF) the observed directional spreading should be directly predicted by the model. It is in this simple case that there is an inconsistency between the models and the observations, and this has a potential impact on the use of the models at all wavenumbers.

Résumé. Les modèles de spectres directionnels de vagues de vent peuvent servir comme outil dans l'interprétation et l'analyse des spectres d'écho Doppler de la mer pour déterminer la direction du vent au-dessus des océans à l'aide de techniques de télédétection. Nous comparons et ajustons l'analyse des données requise en fonction de différentes longueurs d'onde électromagnétique. Pour des nombres d'ondes élevés, l'étalement observé dépend non seulement de l'étalement directionnel du nombre d'ondes de Bragg mais aussi des intégrales pondérées par rapport aux nombres d'ondes plus petits. La discussion concerne les spectres micro-ondes et Doppler VHF. Pour des petits nombres d'ondes (HF), l'étalement directionnel observé devrait être prédit directement par le modèle. Dans ce cas simple, il y a une incohérence entre les modèles et les observations et cela a un impact potentiel sur l'utilisation des modèles indépendamment du nombre d'ondes.
[Traduit par la Rédaction]

Introduction

The determination of wind direction from electromagnetic remote sensing observations over the sea requires an accurate model for spreading parameters in the directional wave spectrum. After over 30 years of work on the directionality of sea waves in the literature, we now have a "best practice" unified model given by Elfouhaily et al. (1997). In this paper the unified model is used to develop the best directional spreading parameters for use in deriving wind direction by electromagnetic remote sensing of the ocean surface.

When the probing wavelength is less than about 1 mm, there is no Bragg resonance and the scattered (or emitted) energy depends on the integrated spectrum of wave slopes. In this case a simple relationship between wind speed and the appropriate spreading parameter can be calculated for the case of infinite fetch.

For the Bragg resonance at high frequency (HF) and longer probing wavelengths we usually get a narrow Bragg "line" (or first-order echo) that is distinct from the modulation energy bands around it. To extract the direction of the wind from these first-order echoes, the spreading parameter appropriate for that particular wavelength must be used. For this case a family of curves is calculated giving the relationship between wind speed and the directional spreading parameter, with the Bragg wavelength generating the family of curves. The effect of fetch is described separately.

When the probing electromagnetic wave has a wavelength below about 2 m, there is often no clear Bragg line in the spectrum. Instead there is a broadened peak where the first-order energy in the Bragg peak is not distinct from the modulation energy introduced by the longer wavelengths. Here the ratio of the positive Bragg "band" of energy to the negative band is often used to determine wind direction. For techniques like scatterometry, which measures the integrated energy, the appropriate spreading parameter is some combination of the value at the Bragg wavelength and an average value over all of the longer wavelengths.

This paper shows how the unified directional spectrum model can be used to improve wind direction determinations for a wide range of remote sensing techniques.

Directional wave spectrum model

A recent review of directional wave spectrum models for wind waves on the sea surface was undertaken by Elfouhaily et al. (1997), who proposed a unified model that retains the Joint North Sea Wave Project (JONSWAP) model at low wavenumbers and a form at high wavenumbers that is constructed to agree with available observations.

Received 1 May 2001. Accepted 21 February 2002.

M.L. Heron. School of Mathematical and Physical Sciences, James Cook University, Townsville 4811, Australia (e-mail: mal.heron@jcu.edu.au).

The model of Elfouhaily et al. (1997) is adapted, so the driving parameters are the wind speed at 10 m elevation (U_{10}, m/s) and fetch (x, m). The directional spectrum model proposed by Elfouhaily et al. is summarized by

$$F(k,\varphi) = \frac{1}{2\pi} k^{-4}(B_l + B_h)G(k,\varphi) \quad (1)$$

where B_l is the low-frequency curvature spectrum, B_h is the high-frequency curvature spectrum, and $G(k, \varphi)$ is the spreading function. The low-frequency term in Equation (1) is

$$B_l = \frac{\alpha_p}{2}\frac{c_p}{c} L_{PM} J_p \exp\left[-\frac{\Omega}{\sqrt{10}}\left(\sqrt{\frac{k}{k_p}} - 1\right)\right]. \quad (2)$$

The Phillips–Kitaigorodskii equilibrium range parameter is

$$\alpha_p = 0.006\sqrt{\Omega} \quad (3)$$

where

$$\Omega = 0.84 \tanh^{-0.75}\left(\frac{X}{X_0}\right)^{0.4} \quad (4)$$

with $X_0 = 22\,000$, and the non-dimensional fetch is $X = gx/U_{10}^2$. The wave celerity at the peak of the gravity wave spectrum is $c_p = (g / k_p)^{1/2}$, and the wavenumber of the gravity wave peak is $k_p = k_0\Omega^2$, where $k_0 = g/U_{10}^2$. The Pierson–Moskowitz (Pierson and Moskowitz, 1964) spectral shape is

$$L_{PM} = \exp\left[-\frac{5}{4}\left(\frac{k_p}{k}\right)^2\right] \quad (5)$$

and the JONSWAP peak enhancement factor is $J_p = \gamma^\Gamma$, where $\gamma = 1.7$ for $0.84 < \Omega < 1$, and $\gamma = 1.7 + 6\ln(\Omega)$ for $1 < \Omega < 5$. Also,

$$\Gamma = \exp\left[\frac{-\left(\sqrt{\frac{k}{k_p}} - 1\right)^2}{2\sigma^2}\right] \quad (6)$$

where $\sigma = 0.08(1 + 4\Omega^{-3})$.

The high-frequency spectral term in Equation (1) is

$$B_h = \frac{\alpha_m}{2}\frac{c_m}{c}\exp\left[-\frac{1}{4}\left(\frac{k}{k_m} - 1\right)^2\right] \quad (7)$$

where $\alpha_m = 0.01[1 + \ln(u^*/c_m)]$ for $u^* < c_m$, and $\alpha_m = 0.01[1 + 3\ln(u^*/c_m)]$ for $u^* > c_m$, and u^* is the friction velocity estimated from the logarithmic boundary layer

$$u^* = \frac{0.42U_{10}}{\ln\left(\frac{10}{z_0}\right)} \quad (8)$$

with roughness length

$$z_0 = 3.7 \times 10^{-5}\left(\frac{U_{10}^2}{g}\right)(c_p U_{10})^{0.9} \quad (9)$$

The spreading function given by Longuet-Higgins et al. (1963) is used in this work:

$$G(\varphi) = A\cos^{2S}\left(\frac{\varphi - \varphi_0}{2}\right) \quad (10)$$

where A is a normalizing factor to make $\int_0^{2\pi} G(\varphi)\mathrm{d}\varphi = 1$ for each value of k and has the form

$$A = \frac{2^{2S-1}\Gamma^2(S+1)}{\pi\Gamma(2S+1)}. \quad (11)$$

The object of the modelling is to be able to estimate the S value at a particular wavenumber and hence determine $(\varphi - \varphi_0)$, the wind direction relative to the "look" direction. **Table 1** shows the constants we have used in the model calculations throughout this work.

Figure 1 shows the elevation spectrum for an infinite fetch and a range of wind speeds, and effectively replicates Figure 8a of Elfouhaily et al. (1997). The energy is higher at nearly all wavenumbers when the wind speed is greater. The wind speed is incremented from 3 m/s to 21 m/s in steps of 2 m/s in the diagram. **Figure 2** illustrates the spreading function $G(\varphi)$ for three selected values of S. The variation of S given by the JONSWAP model is shown in **Figure 3** for infinite fetch. When the fetch is limited the S-values are changed predominantly at low wavenumbers as shown in **Figure 4**.

Table 1. Constants in the directional wave spectrum model.

Gravitational acceleration, g	9.81 m/s
Capillary peak celerity, c_m	0.23 m/s
Capillary peak wavenumber, k_m	361.4/m
Water density, ρ	1025 kg/m
Surface tension, T	0.0740 kg/(m·s^2)

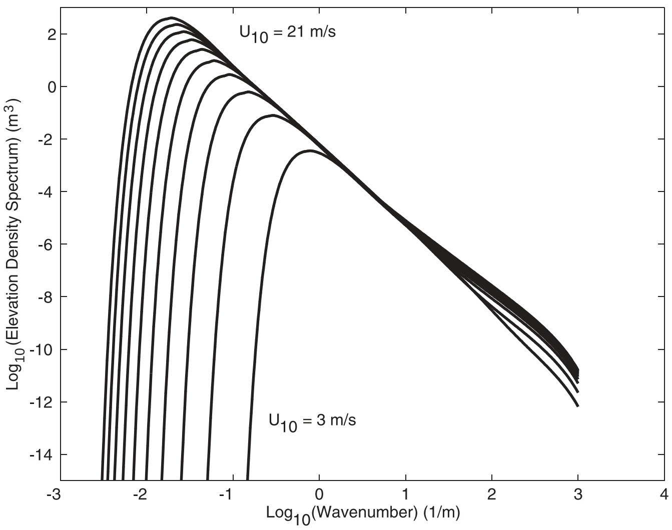

Figure 1. The omni-directional elevation spectrum for a range of wind speeds and for an infinite fetch. The wind speed increases from 3 to 21 m/s in steps of 2 m/s. The low-frequency part of the spectrum is featured at wavenumbers less than about 5/m, and the high-frequency section is seen in the elevations for wavenumbers greater than 5/m.

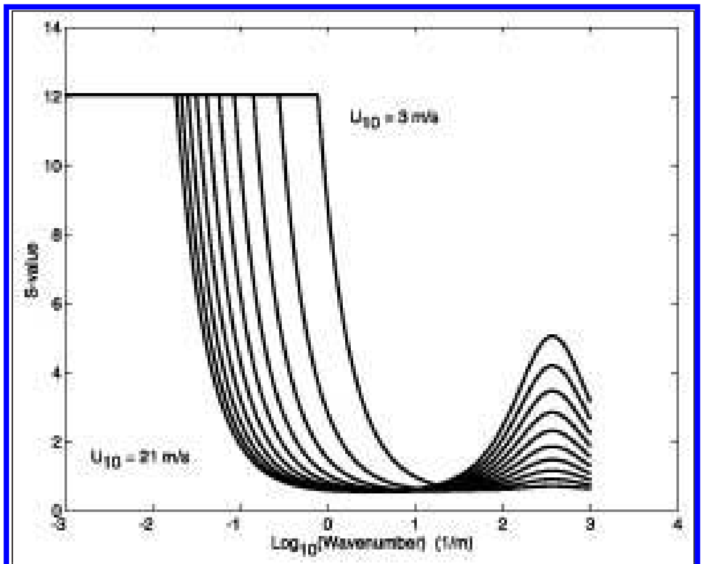

Figure 3. *S* values for the spectrum developed by Elfouhaily et al. (1997). For sea wavenumbers up to about 10, the *S* value is higher for lower wind speeds. For wavenumbers above about 10, this situation reverses and the *S* values are higher for higher wind speeds. These calculations are for infinite fetch.

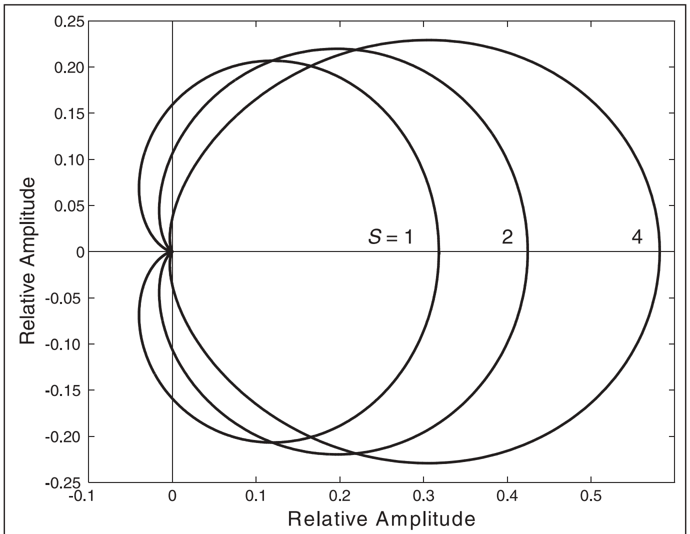

Figure 2. The spreading function suggested by Longuet-Higgins et al. (1963) for S = 1, 2, and 4.

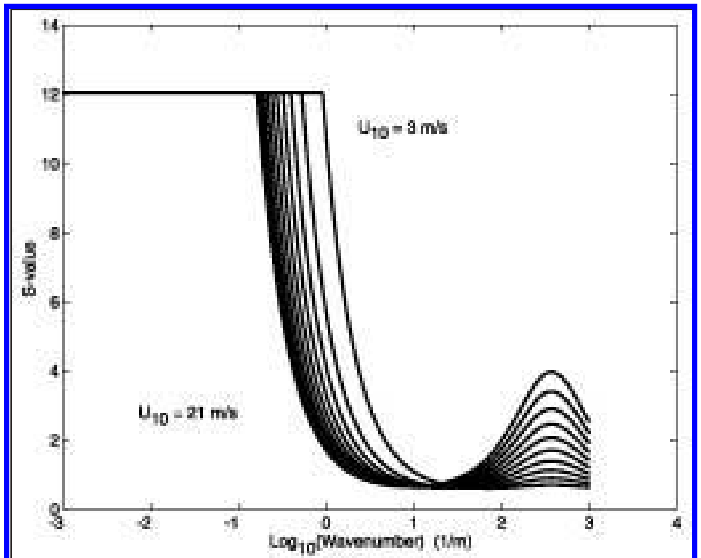

Figure 4. *S* values for the same conditions as those for **Figure 3** except that the fetch is limited to 20 km. In the low-frequency part of the spectrum, the *S* values are higher for a given wavenumber.

Ocean surface radar spectra with Bragg lines

In the HF radar band (3–30 MHz) the backscatter spectrum has a characteristic form with sharp first-order lines at the Bragg frequencies and modulation energy surrounding the Bragg lines. The modulation energy is a combination of second-order spectral lines and a continuum of energy due to interaction between two distinct wave components. Barrick (1972) carried out a synthesis of the HF spectrum by considering the radar wave interacting with a two-dimensional (2D) Fourier description of the ocean surface. A typical HF spectrum is shown in **Figure 5**.

Much work has gone into inverting the HF backscatter spectrum to produce an estimate of the 2D ocean wave spectrum. When this is done it intrinsically contains wind direction and wind speed information in the wave heights and directions of the gravity wind-wave part of the spectrum. Access to this literature can be obtained through Wyatt and Holden (1994). Full inversion requires spectra with good signal-to-noise ratio and the use of two radar sites with beams crossing at the point of study on the sea surface.

A routine analysis method has been developed by Heron and Heron (1998) and Graber and Heron (1997) based on the theoretical work of Barrick (1977), whereby the continuum energy in the modulation sidebands is used to estimate the significant wave height. This provides a wind speed estimate. The ratio of the energy in the two Bragg lines (refer to **Figure 5**) can be used in conjunction with a gravity wave spreading model to determine the wind direction. An example of this procedure is given by Heron and Prytz (2000). This analysis depends on using the ratio of the amplitude of the Bragg waves parallel and anti-parallel to the radar beam. In the HF radar range, the *S* values as a function of wind speed are shown in **Figure 6** for a family of wavenumbers.

The analysis for wind direction from HF backscatter spectra is critically dependent on the accuracy of the spreading model.

Figure 7 shows the same family of curves for a fetch of 20 km. As the fetch increases the peak of the wind wave spectrum moves to higher wavenumbers and the *S* value at the peak increases. Here a fixed wavenumber is being examined where the effect of increasing the fetch in the JONSWAP model is to produce smaller *S* values at a given wind speed.

For completeness, the *S* values were calculated for microwave frequencies where the high-frequency part of the gravity-capillary wave spectrum becomes important. The results in **Figure 8** show *S* increasing with an increase in wavenumber when the wind speed exceeds about 5 m/s. This condition is somewhat unrealistic because, for all but very calm seas, the high modulation on the Bragg lines obliterates the lines and produces a continuum of energy.

Highly modulated scatter from rough sea

For radar wavelengths shorter than about 1 m, the Bragg waves on the sea surface are so heavily modulated that each Bragg line is smeared out into a broadened peak and the integrity of the narrow Bragg line is lost. Under these conditions the surge velocities of the longer wind waves and swell exceed the magnitude of the celerity of the Bragg waves. The consequential frequency modulation of the radar echoes has a modulation index greater than one, in radio engineering terms, and the carrier is indistinguishable from the modulation. When this happens, the energy in each broadened Bragg line is a weighted integral over all waves with longer wavelength than the Bragg wave. The observed spread in directions of the sea surface waves is often measured by the ratio of energy in the broadened Bragg lines. This ratio is insensitive to the

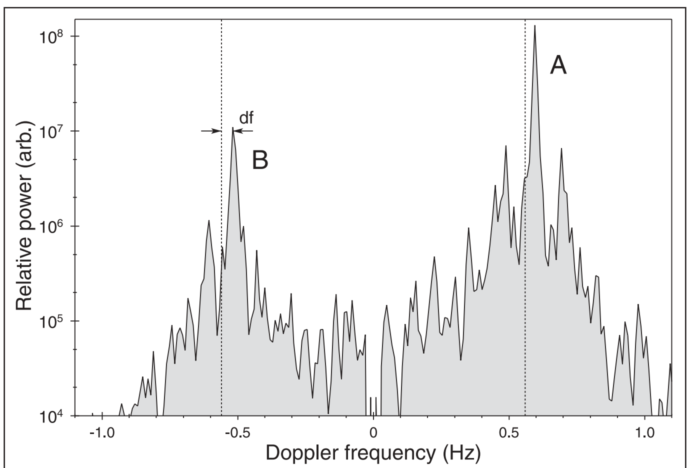

Figure 5. Coastal ocean surface radar system (COSRAD) HF (30 MHz) Doppler spectrum showing Bragg lines with modulation signal clearly separated from the "carrier" signal. There is an offset (df) due to surface current.

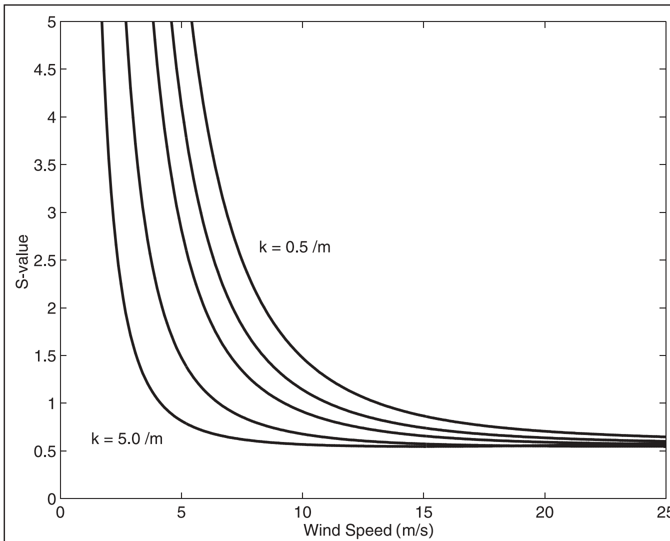

Figure 6. *S* values for the HF radar range of frequencies where the radar spectra have narrow Bragg lines and the analysis is done using the relative energy in the lines. For a given wavenumber, *k*, of the ocean Bragg wave, the *S* value decreases as the wind speed increases. The *k* values in the figure are 0.5, 0.7, 1.0, 2.0, and 5.0/m. The calculations are for infinite fetch.

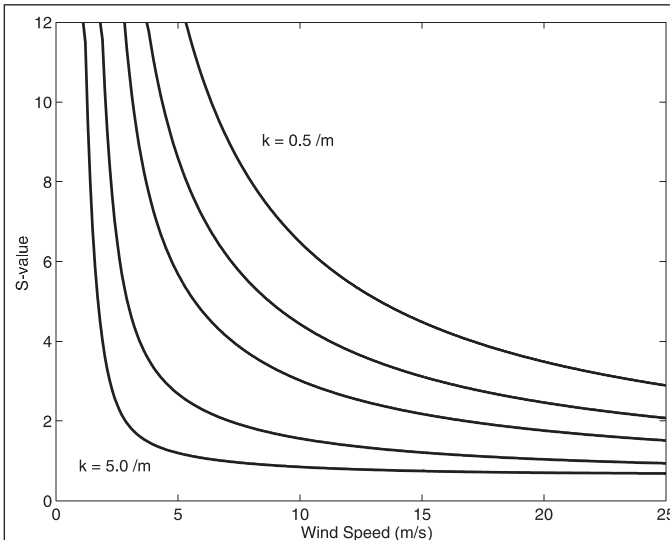

Figure 7. Caption as in **Figure 6** but with a 20 km fetch.

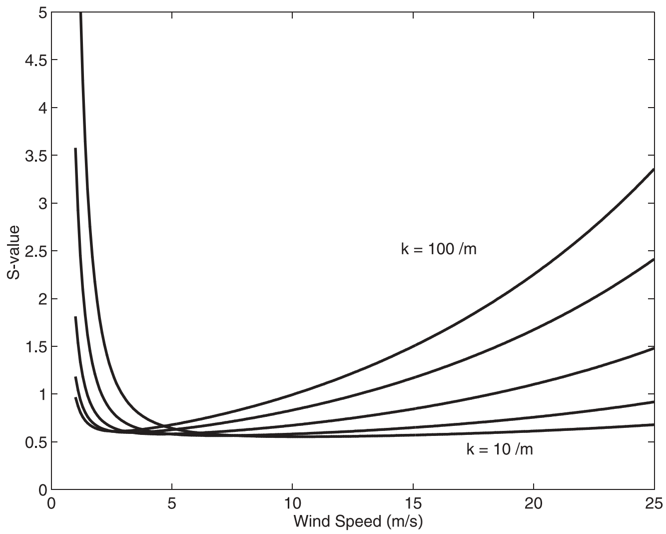

Figure 8. In the microwave radar range, for a given ocean wave Bragg number, the *S* value increases as the wind speed increases for wind speeds above about 5 m/s. The *k* values in the figure are 10, 20, 40, 70, and 100/m.

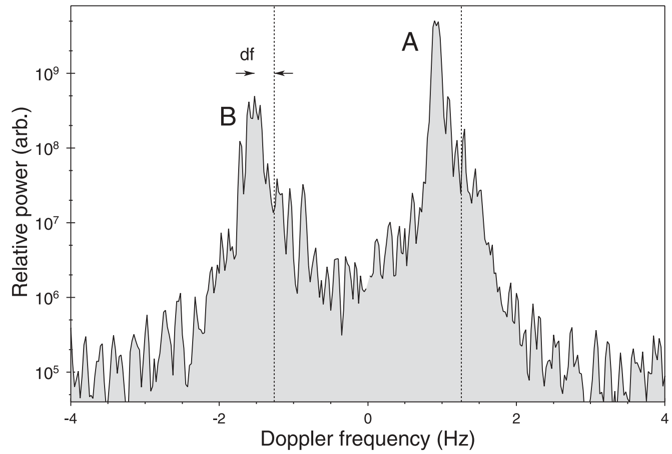

Figure 9. COSRAD VHF (152.2 MHz) Doppler backscatter spectrum showing energy bands at the Bragg frequency locations. The offset (df) is due to surface current.

broadening at HF wavelengths, but as the probing wavelength becomes shorter the ratio is not simply due to the spreading of the Bragg waves on the sea surface but is affected by the longer waves.

An example of this effect is shown in **Figure 9** by a grazing incidence backscatter spectrum in the VHF band at 152.2 MHz. Energy can be seen around the positions of the positive and negative Bragg frequencies, but there are no Bragg spectral lines as in the HF spectrum (**Figure 5**). Here, the frequency modulation produces a continuum of energy and the overall width of the spectral peaks is determined by a combination of sea wave spectral energies for all wavelengths longer than the Bragg wavelength.

A more extreme example is shown in **Figure 10** where the radar frequency is 1.2 GHz. Here the frequency modulation on the echoes due to the underlying long-wavelength waves removes the distinction between the two Bragg energy bands and we are left with a single continuum band of energy. Heron et al. (1996) estimated the frequency modulation by using the JONSWAP model to calculate surge velocities and hence Doppler broadening. The width of the energy band in this experiment was related to the wind speed and wind direction with respect to the radar beam direction.

The relevant spreading function must be weighted over all wavelengths greater than the Bragg wavelength. It is intuitively clear that the weighting will depend on the wave amplitudes and wavelengths on the sea surface. An upper limit on this can be estimated by taking a weighted average of directional spreading and the elevation spectrum over all waves with wavelengths greater than the Bragg wave. The calculation is done for the with-wind and cross-wind directions, and then the weighted average *S* value is obtained.

In the with-wind direction the weighted integral is

$$W_\mathrm{w} = \int_0^{k_\mathrm{Bragg}} F(k)G(k, \theta = 0)\mathrm{d}k \tag{12}$$

where k_Bragg is the Bragg wavenumber; and in the cross-wind direction the weighted integral is

$$W_\mathrm{c} = \int_0^{k_\mathrm{Bragg}} F(k)G(k, \theta = \pi/2)\mathrm{d}k. \tag{13}$$

The integrals were carried out numerically, and the corresponding spreading parameter used by Elfouhaily et al. (1997) is

$$\Delta = \frac{W_\mathrm{w} - W_\mathrm{c}}{W_\mathrm{w} + W_\mathrm{c}} \tag{14}$$

and the weighted average *S* value is

$$S = \frac{1}{\ln 2}\ln\frac{1+\Delta}{1-\Delta}. \tag{15}$$

Some values of *S* calculated by this method are shown in **Figure 11** as a function of wind speed. The two lines are for Bragg wavelengths of 1.0 and 0.05 m. They are very close together and the *S* values are typically around 4.6–5.0.

For scatterometers, it is usually not possible to differentiate between the positive and negative Doppler shifts of Bragg waves propagating towards and away from the radar, respectively. The total received energy from one “look” direction includes both of these, and the observed total energy is compared with that from an orthogonal look direction to determine wind direction. If the *S* value of 4.8 is used in a folded spreading function of the form

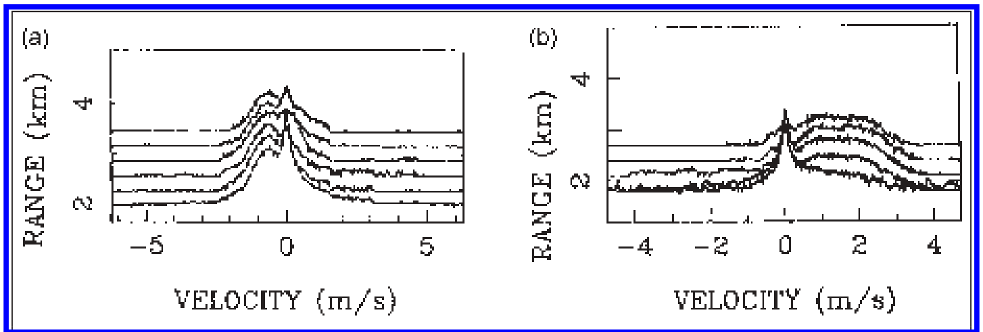

Figure 10. Grazing incidence backscatter at 1.2 GHz showing how the Bragg peaks are overwhelmed by the frequency modulation due to the underlying swell. The graphs show relative power and are staggered on the range axis. Wind speeds are (a) 5.5 m/s at 160° to the radar beam direction, and (b) 5.8 m/s at 10° to the radar beam direction (after Heron et al., 1996).

$$G = A\left[\left|\cos^{2S}\left(\frac{\theta}{2}\right)\right| + \left|\cos^{2S}\left(\frac{\theta+\pi}{2}\right)\right|\right] \quad (16)$$

we get a potentially useful general spreading function for scatterometer analysis. It is outside the scope of this paper to apply this to scatterometer data.

Radiometers

The energy received by radiometers at microwave or infrared wavelengths is affected by the wave slope spectrum because the complex refractive index depends on the local angle of incidence on the water surface. The directionality of the effect is calculated by taking a weighted average of the spreading function over all wavelengths in the slope spectrum. We use the same method to calculate the weighted integrals in the with-wind and cross-wind directions and then find the corresponding S value. The slope spectrum weighted averages are

$$V_{\mathrm{w}} = \int_0^\infty k^2 F(k) G(k, \theta = 0) \mathrm{d}k \quad (17)$$

and

$$V_{\mathrm{c}} = \int_0^\infty k^2 F(k) G(k, \theta = \pi / 2) \mathrm{d}k \quad (18)$$

so

$$\Delta = \frac{V_{\mathrm{w}} - V_{\mathrm{c}}}{V_{\mathrm{w}} + V_{\mathrm{c}}} \quad (19)$$

and the weighted average S value is calculated as in Equation (15). Weighted average S values for the slope spectra for a range of wind speeds are shown in **Figure 12**. The S values are relatively stable around 1.0–2.0 over the wind speed range 3–21 m/s.

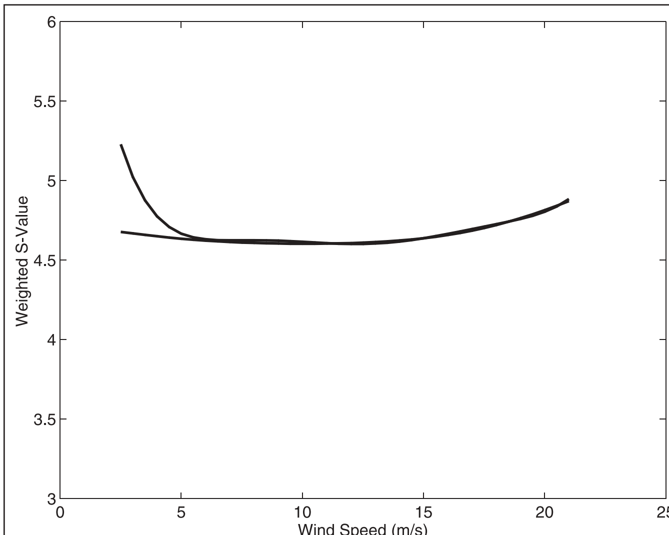

Figure 11. Weighted S values for the elevation spectrum over wavelengths greater than the Bragg wavelengths of 1.00 m (upper line) and 0.05 m (lower line).

Conclusions

In this paper the spreading parameter from a recent unified directional wave spectrum model (Elfouhaily et al., 1997) has been used with the original spreading function suggested by Longuet-Higgins et al. (1963) to evaluate the sensitivity of the S value in a range of remote sensing applications.

The calculations are done for wind speeds in the range 0–25 m/s and mostly for infinite fetch conditions. Three main applications areas are considered and compared. Applications that use Bragg lines to determine sea surface parameters include HF radar and some VHF conditions where the wave spreading function is required only at the Bragg wavenumber. In these cases the S values vary across the range 0.5–12.0 when the wind is in the range 0–25 m/s. Further, the high S values occur at low wind speeds or limited fetch when the wavenumber, k_{p}, of the gravity wave peak is higher. If an S value is to be assumed a priori at the start of analysis, then there are likely to be large errors in the wind direction.

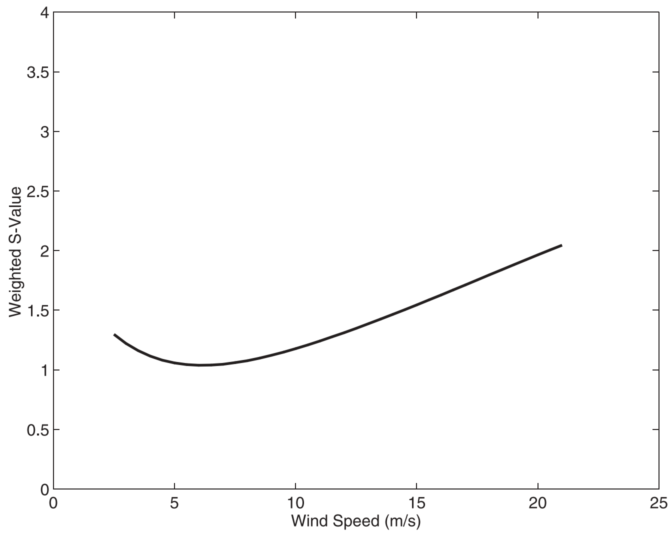

Figure 12. *S* values weighted by the slope spectrum (for all wavenumbers).

There is a different category of applications where the Bragg lines are obliterated by high-level modulation and have spectra which show bands of continuum energy around the Bragg wavenumbers (for VHF spectra), or a single-peaked continuum (for microwave spectra) that obliterates the differentiation between the upper and lower Bragg lines. Analysis in these cases can proceed only by observing the parameters of line broadening and integrated energy. The spreading parameter relevant to these conditions is a weighted integral over all wavenumbers less than the Bragg wavenumber. **Figure 11** shows the *S* values that correspond to the spectral energy (elevation spectrum) in each direction integrated over all wavenumbers in the range $0 < k < k_{\mathrm{Bragg}}$. Except for the very low wind speeds, the *S* values for the elevation spectrum are not sensitive to wind speed and are around 4.6–5.0 for a wide range of Bragg wavenumbers.

Applications that use wavelengths much shorter than the wavelength of the gravity-capillary wave peak sense a directionality which is integrated across the whole sea wave spectrum. For the case of radiometers, it is the directionality of the wave slope spectrum which is relevant, and **Figure 12** shows that the corresponding *S* values lie in the range 1.0–2.0.

The results in **Figures 11** and **12** show that the integration of wave directional spreading effects reduces the dependence of the *S* values on the wind speed. This is true whether it is the elevation spectrum or the wave slope spectrum. For applications that use spectra in which the Bragg lines have been broadened by high-frequency modulation, the *S* values lie in the range $1.0 < S < 2.0$ for slope spectra applications and $4.6 < S < 5.0$ for elevation spectra applications.

When data analysis involves the comparison of energy in a narrow band at the Bragg lines, the range of *S* values is somewhat wider according to the model and caution is needed in the use of an assumed *S* value. Conversely, remote sensing techniques that use relative energies in Bragg lines have good potential to provide reliable *S* values in the range of wavenumbers between the main gravity wave peak and the high-frequency gravity-capillary wave peak. Early work with HF radar (Long and Trizna, 1973; Tyler et al., 1974; Stewart and Barnum, 1975) indicated that *S* values needed to be around 2.0 to get a calibration between wind directions observed by radar and anemometers. More recently, Heron (1987) used HF radar data to show that the *S* values given by the JONSWAP model (K. Hasselmann et al., 1973; D.E. Hasselmann et al., 1980) are too high when k_p is near 1.25/m. These observed low values of *S* are not consistent with the model values shown in **Figures 6** and **7**, or even the weighted values in **Figure 11**.

This inconsistency needs to be resolved because the determination of wind direction at HF depends on the spreading parameters used. Furthermore, there is a potential impact when remotely sensing at higher wavenumbers because the spectrally weighted *S* values depend on the spreading parameters at the low-wavenumber end of the spectrum.

References

Barrick, D.E. 1972. Remote sensing of sea state by radar. In *Remote Sensing of the Troposphere*. Edited by V. Derr. U.S. Government Printing Office, Washington, D.C.

Barrick, D.E. 1977. Extraction of wave parameters from measured HF sea echo Doppler spectra. *Radio Science*, Vol. 12, pp. 415–424.

Elfouhaily, T., Chapron, B., Katsaros, K., and Vademark, D. 1997. A unified directional spectrum for long and short wind-driven waves. *Journal of Geophysical Research*, Vol. 102, 15 781 – 15 796.

Graber, H.C., and Heron, M.L. 1997. Wave height measurements from HF radar. *Oceanography*, Vol. 10, pp. 90–92.

Hasselmann, D.E., Dunckel, M., and Ewing, J.A. 1980. Directional wave spectra observed during JONSWAP 1973. *Journal of Physical Oceanography*, Vol. 10, pp. 1264–1280.

Hasselmann, K., Barnett, T.P., Bouws, E., Carlson, H., Cartwright, D.E., Enke, K. Ewing, J.A., Gienapp, H., Hasselmann, D.E., Kruseman, P., Meerbug, A., Muller, P., Olbers, D.J., Richter, K., Sell, W., and Walden, H. 1973. Measurements of windwave growth and decay during the Joint North Sea Wave Project (JONSWAP). *Deutsch Hydrographische Zeitschrift*, Vol. 12, No. A8 (Suppl.). 93 pp.

Heron, M.L. 1987. Directional spreading of short wavelength fetch-limited wind waves. *Journal of Physical Oceanography*, Vol. 17, pp. 281–285.

Heron, S.F., and Heron, M.L. 1998. A comparison of algorithms for extracting significant wave height from HF radar ocean backscatter spectra. *Journal of Atmospheric and Oceanic Technology*, Vol. 15, pp. 1157–1163.

Heron, M.L., and Prytz, A. 2000. Wind speed and direction from the HF coastal ocean surface radar. In *Proceedings of the OceanWinds2000 Workshop*, IFREMER, Brest, France.

Heron, M.L., Nadai, A., and Masuda, Y. 1996. An estimate of Doppler frequency shift and broadening for grazing incidence C-band ocean surface backscatter. In *PORSEC, Proceedings of the Pacific Ocean Remote Sensing Conference*, 12–16 August 1996, Victoria, B.C. PORSEC 1996 Secretariat, Institute of Ocean Sciences. pp. 151–159.

Long, A.E., and Trizna, D.B. 1973. Mapping of North Atlantic winds by HF radar sea backscatter interpretation. *IEEE Transactions on Antennas and Propagation*, Vol. AP-21, pp. 680–685.

Longuet-Higgins, M.S., Cartwright, D.E., and Smith, N.D. 1963. Observations of the directional spectrum of sea waves using the motion of a flotation buoy. In *Proceedings of the Conference on Ocean Wave Spectra*. Prentice-Hall Inc., Englewood Cliffs, N.J. pp. 111–136.

Pierson, W.J., and Moskowitz, L. 1964. A proposed spectral form for fully developed wind sea based on the similarity theory of S.A. Kitaigorodskii. *Journal of Geophysical Research*, Vol. 69, pp. 5181–5190.

Stewart, R.H., and Barnum, J.R. 1975. Radio measurements of oceanic winds at long ranges: an evaluation. *Radio Science*, Vol. 10, pp. 853–857.

Tyler, G.L., Teague, C.C., Stewart, R.H., Munk, A.M., and Joy, J.W. 1974. Wave directional spectra from synthetic aperture observations of radio scatter. *Deep Sea Research*, Vol. 21, pp. 989–1016.

Wyatt, L.R., and Holden, G.J. 1994. HF radar measurement of multimodal directional wave spectra. *Global Atmosphere and Ocean System*, Vol. 2, pp. 265–290.